https://doi.org/10.1007/s41230-026-4124-6

Influence of mold wall thickness on morphologies of defect band in high-pressure die casting technology

Zhen-yu Sun[1], *Wen-bo Yu[1], Jun-jie Li[1], Wei-chen Zheng[1], Guang-rui Wang[1], Jian-ru Fang[2], and **Shou-mei Xiong[3]

1. Center of Materials Science and Engineering, School of Mechanical and Electronic Control Engineering, Beijing Jiaotong University, Beijing 100044, China

2. Dalian Yaming Auto Parts Co., Ltd., Dalian 116041, Liaoning, China

3. School of Materials Science and Engineering, Tsinghua University, Beijing 100084, China

Abstract: In order to investigate the effect of die wall thickness on morphologies of defect band, a stepped mold with a wall thickness of 5 mm, 4 mm, 3 mm, 2 mm, and 1 mm was designed to carry out high pressure die casting experiments with AlSi10MgMn alloy. For castings with wall thickness of 2–4 mm, the ratio of the mean defect band width (w) and mean grain size (d) in the defect band (w/d) ranges 7–18, while it increases to 24.47 for the 5 mm-thick casting. This difference is related with the filling speed and the distribution of externally solidified crystals (ESCs). The mold flow analysis indicates that the filling speed decreases from 25.41 $m \cdot s^{-1}$ to 11.07 $m \cdot s^{-1}$ when wall thickness increases from 2 mm to 5 mm. Due to the decreasing filling speed along the wall thickness, ESCs gradually diffuse from the center to the defect band, which keep the shear strength in the defect band at a high-level during filling. Meanwhile, the shear strength generated during the filling also decreases as the shear rate drops. Finally, the defect bands in the 5 mm-thick region become widen and indistinct, and the porosity is as high as 5.25%.

Keywords: AlSi10MgMn; high pressure die casting; defect band; mold flow analysis; externally solidified crystals

CLC numbers: TG146.21 **Document code:** A **Article ID:** 1672-6421(2026)01-031-06

1 Introduction

The ultra-large integrated high pressure die casting (HPDC) technology equipped with large and complex molds is currently the first choice for achieving efficient near-net forming of complex lightweight aluminum alloy structural parts. It has good forming ability, high production efficiency, and good economic index, which is suitable for mass manufacturing of large-scale parts[1, 2]. HPDC contains different process parameters and the ultra-large integrated die inevitably contains different wall thicknesses. The microstructure of die castings must be influenced by uneven wall thickness and the relative study should have been and being conducted.

Defect band, as one of the representative features in HPDC castings, is often observed in outer contour of castings. Hou et al.[3] reported that macrosegregation and porosities exist in defect band, which is detrimental to the mechanical properties of castings. Dahle and StJohn[4] reported that the formation of defect band was closely related to the rheological and solidification behavior in the mushy zone. Li et al.[5] proposed that the shear stress developed during both filling and subsequent solidification processes was particularly important for the formation of defect band. Furthermore, Gourlay et al.[6] found that the formation of defect band was independent of ESCs, which had been confirmed by the experiments of Rodrigo and Ahuja[7]. But the presence and distribution of ESCs might influence mush rheology during filling and feeding to indirectly affect defect band formation. For example,

***Wen-bo Yu**

Ph. D., Research interests: Microstructural control and regulation of rapid solidification, including die-casting, laser cladding, and spraying.

E-mail: wbyu@bjtu.edu.cn

****Shou-mei Xiong**

E-mail: smxiong@tisnghua.edu.cn

Received: 2024-10-07; Revised: 2025-01-08; Accepted: 2025-01-13

Niu et al.[8] reported that ESCs could impede flow through the gates and thus influence filling and feeding. Gourlay et al.[9] found that the position of the defect band would move toward the die wall with increasing die temperature and external fraction solid f_s^{ESC}. Jiao et al.[10] found that owing to the constraining relationship among the process parameters, complete avoidance of the ESCs in the microstructure of die castings seemed impossible. While, Laukli et al.[11] and Dinnis et al.[12] reported that the location and morphology of the defect band were influenced by the Si content, and the defect band width could be well reduced by decreasing Si content in Al-Si alloy. Yu et al.[13] systematically studied the influence of die-casting process on defect band width and proposed that the defect band width was strongly proportional with the size and quantities of ESCs. Jiao et al.[2] reported that increasing slow shot speed can make the defect band more obvious and closer to the center. While, there is still lack of the systematic research about the effect of wall thickness on the microstructure about HPDC castings, especially on the defect band.

Based on the above discussion, in order to study the effect of wall thickness on defect bands, the stepped castings were produced by a stepped mold with the wall thicknesses of 1 mm, 2 mm, 3 mm, 4 mm, and 5 mm. By microstructural characterization and mold flow analysis, the influence of ESCs distribution and the shear stress generated by the filling speed on defect band formation was elucidated. In addition, 3D characterization was conducted to analyze the porosity distribution in castings.

2 Experiment

Figure 1(a) shows the geometric model of the high pressure die casting produced. Figure 1(b) shows the main view and top view of the stepped casting with steps of 5 mm, 4 mm, 3 mm, 2 mm, and 1 mm thick in the filling direction from left to right. The red box regions in Fig. 1(b) were used for the 3D reconstruction experiment, and the specific dimensions are shown in Fig. 1(c). The location of metallographic sample is shown in Fig. 1(d), which means removing the remaining part of the 3D reconstruction region and observing the yellow region on the surface. The actual composition of AlSi10MgMn alloy used in this experiment is shown in Table 1.

The stepped castings were prepared by cold chamber HPDC TOYO-BD-350V5 from Changchun FAW Casting Co. Ltd. The total length and diameter of the injection sleeve were 340 mm and 70 mm, respectively. It was equipped with a vacuum system and a casting pressure of 13.7 MPa was applied at the location of 285 mm in injection sleeve. The specific die casting process is shown in Table 2. The pouring temperature was 695 °C and the mold preheating temperature was 150 °C.

The obtained castings were ground and polished. The microstructure in each thickness region of the stepped castings was observed using optical microscopy (OM) and scanning electron microscopy (SEM). In addition, 3D reconstruction was also applied to characterize and analyze the porosities of the castings. In response to the phenomenon of significant differences in porosity distribution in the 5 thickness regions,

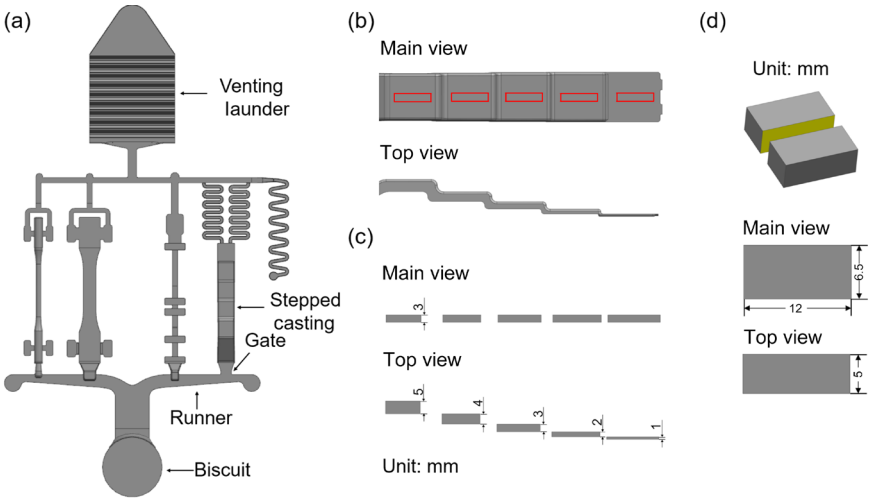

Fig. 1: Configuration of HPDC casting (a), stepped casting (b), samples for synchrotron radiation experiment (c), and location for metallographic samples (d)

Table 1: Chemical composition of AlSi10MgMn alloy (wt.%)

Si	Fe	Cu	Mn	Mg	Zn	Ti	Sr	Al
10.13	0.14	0.02	0.59	0.28	0.24	0.07	0.01	Bal.

Table 2: Details of HPDC process parameters

Low slow-shot speed 1 ($m \cdot s^{-1}$)	Position	Low slow-shot speed 2 ($m \cdot s^{-1}$)	Position	Fast slow-shot speed ($m \cdot s^{-1}$)	Position
0.2	80	0.1	120	1.5	270

the filling and solidification processes of stepped samples were simulated by SupreCAST to explain this phenomenon.

3 Results

Figures 2(a–e) show the cross-sectional microstructure along the flow direction of the AlSi10MnMg castings with the wall thickness of 1–5 mm. The marked regions of I–V were further enlarged. It can be seen the defect bands contain white ESCs, gray eutectic Si, white primary α-Al grains, and black pores. For the step of 1 mm, a large number of pores appear and the defect band is not visible. This phenomenon is aroused by the air entrapment caused by the inappropriate mold design. The defect band widths decrease with the decreasing thickness of steps. In the 2–5 mm wall thickness regions, the measured defect band widths are 102.48 μm, 127.57 μm, 175.37 μm, and 258.53 μm, respectively. More importantly, in the 2–4 mm wall thickness regions, ESCs are observed to distribute along the defect bands. In contrast, in the 5 mm wall thickness region, ESCs penetrate into the interior of defect band.

Figure 3 presents the mold flow analysis obtained by SupreCAST. As shown in Fig. 3(a), the contact region between the step region and venting channel is so limited that the air can not be effectively evaculated. The serious gas entrapment occurs and the high gas porosity quantity subsequently is found in the 1 and 2 mm-thick regions, especially in the 1 mm-thick region. As shown in Fig. 3(b), the filling speed increases from 11.07 $m \cdot s^{-1}$ to 34.15 $m \cdot s^{-1}$ with the decreasing wall thickness from 5 mm to 1 mm. The fast-filling speed arouses the flow turbulent at the 1 mm-thick region, which strongly disperses the entrapped pores and disorders the microstrucutre. Fortunately, the defect bands in 2–5 mm wall thickness regions are not disturbed and are taken for the following investigation. The thinnest part of inner gate is only 3.3 mm, which is thinner than the step of 5 mm. As shown in Fig. 3(c), the metal flow in inner gate solidifies earlier than the step of 5 mm. Even though the entrance of liquid feeding is cut off, the defect band region is not influenced in the 5 mm wall thickness region. As shown in Fig. 2(e), a large amount of shrinkage pores appear in the center of the 5 mm wall thickness region.

Regarding the solidification characteristics during HPDC, the porosity defect resulting from air entrapment and solidification shrinkage is inevitable as that reported by Zhang et al[14] and Li et al[15]. Figure 5 presents the 3D reconstruction of shrinkage pores in the 1–5 mm wall thickness regions. The porosities in the steps from 1 mm to 5 mm are 6.98%, 4.96%, 2.72%, 2.52%, and 5.25%, respectively. As

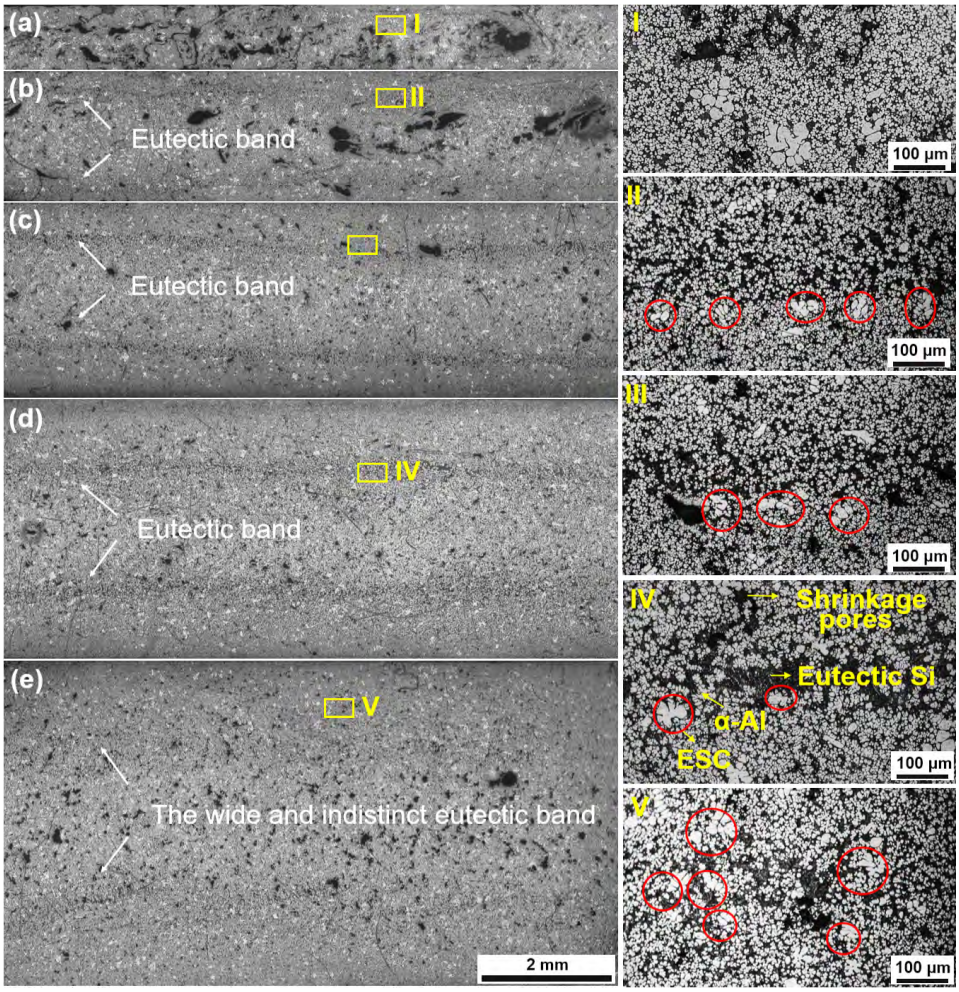

Fig. 2: Optical micrographs in 1–5 mm-thick regions (a–e), and higher magnification micrographs corresponding to marked regions in (a–e) (I–V)

shown in Fig. 4, the 1 mm and 2 mm wall thickness regions are influenced by serious gas entrapment caused by the thin venting channel, so the porosities in 1 mm and 2 mm wall thickness regions are high. For 3–5 mm wall thickness regions, the distribution of shrinkage pores spreads from the center to the defect band with the increasing wall thickness. In particular, the defect band in the 5 mm wall thickness region presents significant shrinkage pores enrichment. Ma et al.[16] reported that the shrinkage pores are strongly related with ESCs. The ESCs would gradually form an interlocking rigid dendritic network during the solidification process. As shown in Fig. 2(V), a large number of ESCs spread into the defect band in the 5 mm wall thickness region. The shrinkage pores would form in the defect band because of the difficult metal liquid feeding. Differently, the ESCs in the 3 mm and 4 mm wall thickness regions do not spread into the defect bands, therefore, no accumulated shrinkage pores appear in their defect bands.

4 Discussion

Otarawanna et al.[17] reported that the ratio of the mean defect band width to mean grain size (w/d) in the defect band was measured to be in the range 7–18. This range is one index that the formation of defect bands is resulted from the strain localization in partially solidified alloys during HPDC. Therefore, the defect band width in the 1–5 mm wall thickness regions was measured. Optical micrographs in the etched condition were used to measure defect band thicknesses and grain size in this work, because macrosegregation is well revealed by etching and the relatively high resolution of optical microscopy[17]. Due to the significant impact of ESCs on the width and grain size of defect band regions, measurements of defect band width and grain size must be taken in defect band regions containing no ESCs. For example, both Fig. 5(I) and Fig. 5(II) were taken from the defect band, Fig. 5(I) should be used for measurement while Fig. 5(II) should be discarded.

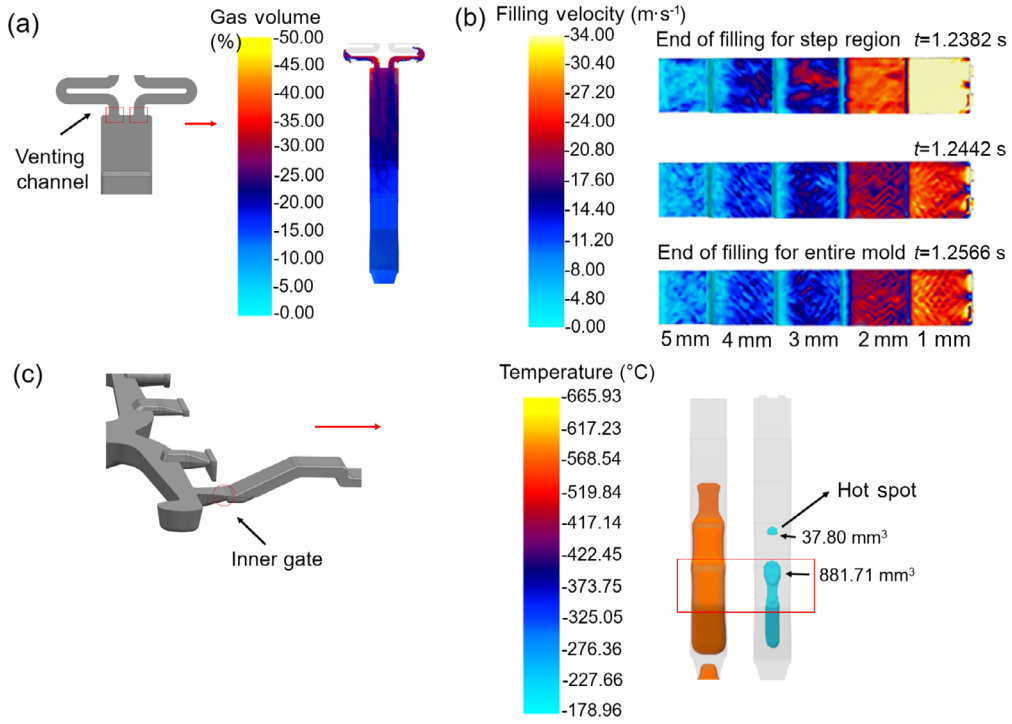

Fig. 3: Venting channel and gas volume in casting (a), filling velocity in casting (b), and inner gate and simulation of solidification process (c)

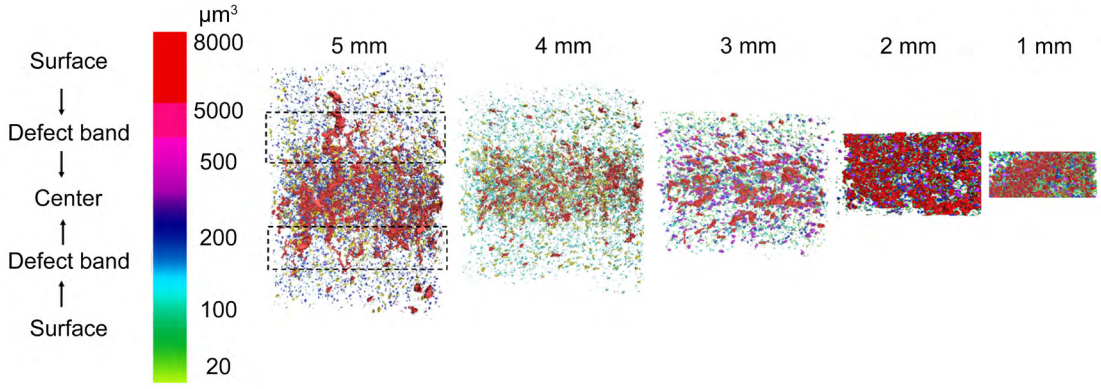

Fig. 4: 3D reconstruction of shrinkage pores from surface to center, the steps of 5 mm, 4 mm, 3 mm, 2 mm, and 1 mm from left to right

Figure 6 plots the curves of the mean defect band width and mean grain size in the defect band. The measured *w*/*d* for the defect bands in 2–4 mm wall thickness regions are in the range of 7–18. However, the *w*/*d* in the 5 mm wall thickness region is about 24.47, which is beyond the range of 7–18.

Gourlay et al.[9] reported that high filling speed facilitates ESCs accumulation into the casting centerline, as ESCs tend to migrate towards the lower shear rate region during die filling. As shown in Figs. 2(II–V), the ESCs are generally distributed along the defect band boundaries in the 2–4 mm wall thickness regions. According to the simulation of filling process shown in Fig. 3(b), the metal filling speed decreasea from 25.41 m·s^{-1} to 11.07 m·s^{-1} with decreasing wall thickness from 2 mm to 5 mm. The low filling speed in the 5 mm wall thickness region can not produce the enough strong shear stress for migrating ESCs to the casting center. Therefore, ESCs begin to spread into the defect band in the 5 mm wall thickness region, as shown in Fig. 2(V).

The ESCs within the defect band of the 5 mm wall thickness region further influence the formation of the defect band. The theory proposed by Dahle and StJohn[4] supported that the dendrites coherency solid fraction (f_s^{coh}) indicates the appearance of shear strength. Once the solid fraction (f_s) in mush zone reaches the maximum packing solid fraction (f_s^{pk}), the shear strength of mush zone would increase more rapidly. Figure 7 shows that the values of f_s^{coh} and f_s^{pk} are strongly related with the grain size and morphology in the mushy zone. In comparison with the mushy zone containing small globular grains, the values of f_s^{coh} and f_s^{pk} are much smaller for the mushy zone containing large dendrites. According to the Figs. 2(II–IV), as almost no ESCs are involved into the defect bands in the 2–4 mm wall thickness regions, the grains in the defect bands are mostly equiaxed and small. However, according to the Fig. 2(V), the solid fraction in defect band is strongly increased in the filling stage due to the involvement of ESCs in the 5 mm wall thickness region. As shown in Fig. 7, the f_s^{coh} and f_s^{pk} in defect band of the 5 mm wall thickness region would be reach earlier in comparison with the 2–4 mm wall thickness regions.

The formation of shear defect band is not only influenced by ESCs, but also by the shear strength, and the shear strength is strongly related with the filling speed[4]. According to the simulation of filling process shown in Fig. 3(b), the filling speed decreases from 25.41 m·s^{-1} to 11.07 m·s^{-1} from the 2 mm

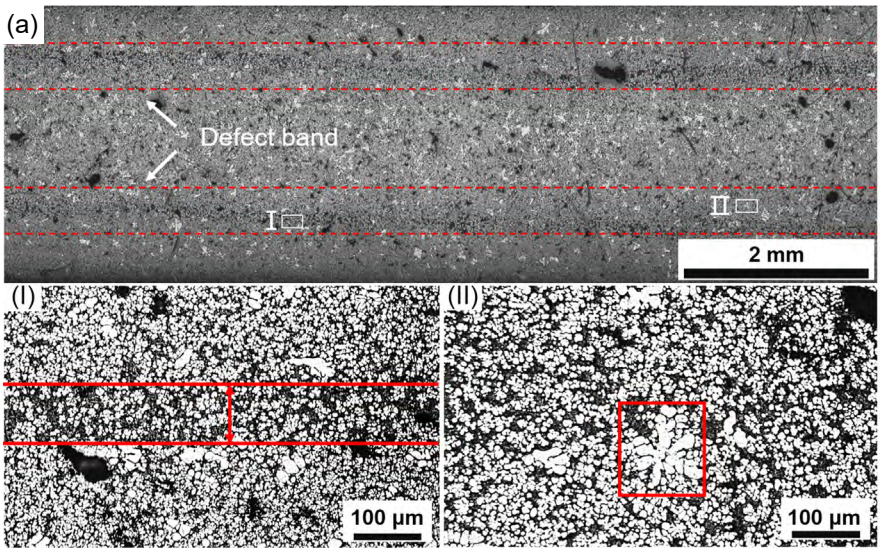

Fig. 5: Optical micrograph of 3 mm wall thickness region (a), (I) is defect band containing no ESCs taken from the defect band in (a), (II) is defect band containing ESCs taken from the defect band in (a)

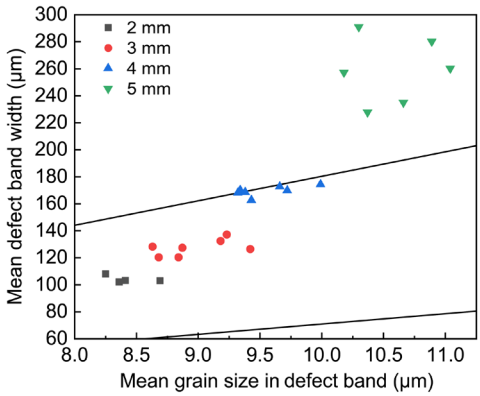

Fig. 6: Relationship between mean defect band width and mean grain size in the defect band for different wall thickness regions

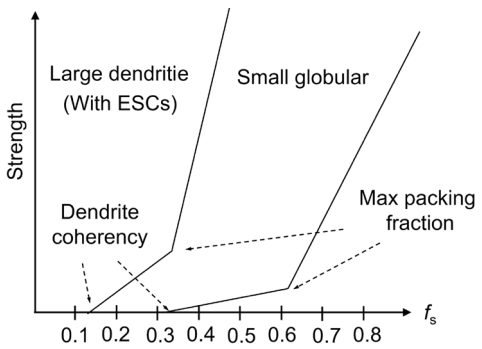

Fig. 7: Increase of shear strength vs solid fraction in the mushy zone for two extremes in microstructures: large dendritic grains and small globular grains, which was reported by Dahle and StJohn[4]

to 5 mm wall thickness regions. Herein, the shear strength produced by the filling liquid metal decreases and reaches the lowest in the 5 mm wall thickness region. However, among all the regions, the f_s in the defect band of the 5 mm wall thickness region firstly approaches to f_s^{coh} and f_s^{pk} because of the large ESCs involvement. The strength of mushy zone in the 5 mm wall thickness region significantly increases. Finally, because of the insufficient shear strength caused by the relatively low filling speed and high content of ESCs in metal liquid, a wide and indistinct defect band appears in the 5 mm wall thickness region. Its corresponding *w*/*d* exceeds the range of 7–18. For the other 2 mm to 4 mm wall thickness regions, the globular grain size is relatively small because almost no ESCs penetrate the defect bands. The threshold value of f_s^{coh} is higher and the strength of defect bands develops more slowly. Meanwhile, the shear stress generated by the filling speed is higher, especially with the decreasing step thickness. Therefore, their defect bands are more distinct and their *w*/*d* values are in the range of 7–18.

5 Conclusion

In order to investigated the influence of wall thickness on the morphology of defect band, AlSi10MgMn alloy was cast by HPDC equipped with one stepped die containing different thicknesses (1 mm, 2 mm, 3 mm, 4 mm, and 5 mm). The 1 mm wall thickness region is not taken into consideration because of serious gas entrapment. For the 2–5 mm wall thickness regions, the width of defect band (*w*) and grain size (*d*) in the defect bands were measured. The ratio of *w*/*d* in the 2–4 mm wall thickness regions are in the range of 7–18. However, the *w*/*d* in the 5 mm wall thickness region is 24.47, which is beyond the range of 7–18. The microstructural characterization and mold flow analysis confirm that the distribution of ESCs is strongly related with the shear strength in mushy zone. The shear strength is further decided by metal filling rate influenced by step thickness. ESCs are distributed along the boundaries in the 2–4 mm wall thickness regions, while they are involved into defect band in the 5 mm wall thickness region. Once ESCs are involved into defect band, defect band becomes widen and indistinct. Meanwhile, the involvement of ESCs into the defect band further facilitates the formation of shrinkage pores. This study confirms that the reduction of ESCs is the key factor for reducing the defect band width and the shrinkage porosity within the defect band.

Acknowledgments

This work was supported by the National Natural Science Foundation of China (No. 52474396 and 52175284) and the National Key Research and Development Program of China (Grant No. 2022YFB3404201). Thanks to the technical support of BL13W1 beamline in Shanghai Synchrotron Radiation Facility (SSRF) and Gaomi Xiangyu company.

Conflict of interest

The authors declare that they have no conflict of interest.

References

[1] Luo A A, Sachdev A K, Apelian D. Alloy development and process innovations for light metals casting. Journal of Materials Processing Technology, 2022, 306: 117606.
[2] Jiao X Y, Wang P Y, Liu Y X, et al. Effect of shot speeds on the microstructural framework and abnormal eutectic bands in a high pressure die casting hypoeutectic AlSi10MnMg alloy. Journal of Materials Processing Technology, 2024, 326: 118312.
[3] Hou Y Y, Wu M W, Huang F, et al. Defect band formation in high pressure die casting AE44 magnesium alloy. China Foundry, 2022, 19(3): 201–210.
[4] Dahle A K, StJohn D H. Rheological behaviour of the mushy zone and its effect on the formation of casting defects during solidification. Acta Materialia, 1998, 47(11): 31–41.
[5] Li X, Xiong S M, Guo Z. On the tensile failure induced by defect band in high pressure die casting of AM60B magnesium alloy. Materials Science and Engineering: A , 2016, 674: 687–695.
[6] Gourlay C M, Laukli H I, Dahle A K. Defect band characteristics in Mg-Al and Al-Si high-pressure die castings. Metallurgical and Materials Transactions: A, 2007, 38: 1833–1844.
[7] Rodrigo P D D, Ahuja V. Effect of casting parameters on the formation of 'pore/segregation bands' in magnesium die castings. Magnesium 2000 – 2nd Israeli Conf, on Magnesium Science and Technology, 2000: 97–104.
[8] Niu X P, Tong K, Hu B H. Cavity pressure sensor study of the gate freezing behaviour in aluminium high pressure die casting. International Journal of Cast Metals Research, 2016, 11(2): 105–112.
[9] Gourlay C M, Dahle A K, Laukli H I. Segregation band formation in Al-Si die castings. Metallurgical and Materials Transactions: A, 2004, 35: 2881–2891.
[10] Jiao X Y, Zhang Y F, Wang J. Characterization of externally solidified crystals in a high-pressure die-cast AlSi10MnMg alloy and their effect on porosities and mechanical properties. Journal of Materials Processing Technology, 2021, 298: 117299.
[11] Laukli H I, Gourlay C M, Dahle A K. Effects of Si content on defect band formation in hypoeutectic Al-Si die castings. Materials Science and Engineering: A, 2005, 413–414: 92–97.
[12] Dinnis C M, Dahle A K, Taylor J A. Three-dimensional analysis of eutectic grains in hypoeutectic Al-Si alloys. Materials Science and Engineering: A, 2005, 392(1–2): 440–448.
[13] Yu W B, Ma C S, Ma Y H. Correlation of 3D defect-band morphologies and mechanical properties in high pressure die casting magnesium alloy. Journal of Materials Processing Technology, 2021, 288: 116853.
[14] Zhang Y J, Lordan E, Dou K. Influence of porosity characteristics on the variability in mechanical properties of high pressure die casting (HPDC) AlSi7MgMn alloys. Journal of Manufacturing Processes, 2020, 56: 500–509.
[15] Li X, Xiong S M, Guo Z. On the porosity induced by externally solidified crystals in high-pressure die-cast of AM60B alloy and its effect on crack initiation and propagation. Materials Science and Engineering: A, 2015, 633: 35–41.
[16] Ma C S, Yu W B, Zhang T T. The effect of slow shot speed and casting pressure on the 3D microstructure of high pressure die casting AE44 magnesium alloy. Journal of Magnesium and Alloys, 2023, 11(2): 753–761.
[17] Otarawanna S, Gourlay C M, Laukl H I. The thickness of defect bands in high-pressure die castings. Materials Characterization, 2009, 60(12): 1432–1441.
[18] Han Q, Zhang J. Fluidity of alloys under high-pressure die casting conditions: Flow-choking mechanisms. Metallurgical and Materials Transactions: B, 2020, 51: 1795–1804.